

# Deshraj Meena

## Enhanced Thermoelectric Properties of Tin Selenide-Based Flexible Polymer Composites

 Phd Scholars

---

### Document Details

Submission ID

trn:oid:::27535:140620842

Submission Date

May 27, 2026, 12:02 PM GMT+5:30

Download Date

May 27, 2026, 12:16 PM GMT+5:30

File Name

Enhanced Thermoelectric Properties of Tin Selenide-Based Flexible Polymer Composites.pdf

File Size

2.1 MB

33 Pages

4,712 Words

24,629 Characters

AI  
28-05-2026

# 3% Overall Similarity

The combined total of all matches, including overlapping sources, for each database.

## Filtered from the Report

- ▶ Small Matches (less than 10 words)

## Match Groups

- 8 Not Cited or Quoted 3%**  
Matches with neither in-text citation nor quotation marks
- 0 Missing Quotations 0%**  
Matches that are still very similar to source material
- 0 Missing Citation 0%**  
Matches that have quotation marks, but no in-text citation
- 0 Cited and Quoted 0%**  
Matches with in-text citation present, but no quotation marks

## Top Sources

- 1% Internet sources
- 2% Publications
- 2% Submitted works (Student Papers)

## Integrity Flags

0 Integrity Flags for Review

Our system's algorithms look deeply at a document for any inconsistencies that would set it apart from a normal submission. If we notice something strange, we flag it for you to review.

A Flag is not necessarily an indicator of a problem. However, we'd recommend you focus your attention there for further review.

## Match Groups

- 8 Not Cited or Quoted 3%**  
Matches with neither in-text citation nor quotation marks
- 0 Missing Quotations 0%**  
Matches that are still very similar to source material
- 0 Missing Citation 0%**  
Matches that have quotation marks, but no in-text citation
- 0 Cited and Quoted 0%**  
Matches with in-text citation present, but no quotation marks

## Top Sources

- 1% Internet sources
- 2% Publications
- 2% Submitted works (Student Papers)

## Top Sources

The sources with the highest number of matches within the submission. Overlapping sources will not be displayed.

<b>1</b>	Publication	Chung, . "Introduction to Functional Materials and their Applications", Functional...	<1%
<b>2</b>	Student papers	University of Queensland on 2016-10-07	<1%
<b>3</b>	Publication	Krushna K. Raut, Raju Chetty, Jayachandran Babu, Andrei Novitskii, Vikrant Trived...	<1%
<b>4</b>	Student papers	University of Witwatersrand on 2024-09-15	<1%
<b>5</b>	Student papers	Higher Education Commission Pakistan on 2010-04-07	<1%
<b>6</b>	Publication	Rui Yang, Jiacan He, Jing Wang, Xin Xue, Guirong Zhou, Zhaohui Song, Yi He, Xiao...	<1%
<b>7</b>	Publication	Yiren Xiong, Guoqiang Guo, Hongyi Xian, Zuqing Hu et al. "MCF-7 cell - derived ex...	<1%
<b>8</b>	Internet	www.mdpi.com	<1%

# CHAPTER 1

## 1.1 INTRODUCTION

With the increase in the industrial revolution in the past couple decades, unprecedented amounts of energy are getting wasted. This calls for the betterment of the technologies for the replenishment of waste heat and the need for the development of such methods through which waste heat can be reused [1]. Thermoelectricity is one such method through which thermal energies can be converted into electrical energies and vice versa. Via thermoelectric materials realization of mutual conversion between heat and electricity is possible. This has made thermoelectric materials an emerging research topic [2]. The conversion of thermal energy into electrical energy is known as the Seebeck effect and its counterpart that is the conversion of electrical energy into heat energy is known as the Peltier effect.

The performance or the effectiveness of a thermoelectric material can be measured using the thermoelectric figure of merit or the thermoelectric efficiency  $ZT$ , which can be described as,[3]

$$ZT = \frac{S^2 \sigma}{k} T$$

$ZT$  is the dimensionless figure of merit

$S$  is the Seebeck coefficient

$\sigma$  is the electrical conductivity

$k$  is the thermal conductivity

$T$  is the absolute temperature

The thermoelectric power factor is given by the product  $S^2 \sigma$  and this depicts the thermopower of the material [4].

The thermal conductivity  $k$  is given by the formula, [5]

$$k = k_e + k_p$$

$$k_e = L \sigma T$$

where,  $k_e$  represents the electronic thermal conductivity and  $k_p$  represents the lattice thermal conductivity which is due to the phonon distribution and  $L$  is the Lorentz factor [5].

3 The electrical conductivity is given by the formula, [6]

$$\sigma = ne\mu$$

where,  $n$  represents the carrier concentration,  $e$  represents the electronic charge and  $\mu$  represents the carrier mobility [6].

The Seebeck Coefficient measures the voltage generated upon a temperature gradient and can be described by [7,8],

$$S = \frac{\Delta V}{\Delta T} = \frac{8\pi^2 k_B^2 m^* T}{3eh^2} \left(\frac{\pi}{3n}\right)^{\frac{2}{3}}$$

To produce a thermoelectric material with a high figure of merit, we need to optimize these factors because of their interdependence over each other.

**Tin Selenide (SnSe):** Tin Selenide is one of the many promising thermoelectric materials due to its properties like low toxicity, cost-effectiveness and a high thermoelectric figure of merit obtained from its semi-conductor like bandgap of around 0.9 eV and low value of intrinsic lattice thermal conductivity ( $k_l$ ) [9,10].

Out of the bulk materials based on Tin Selenide, the highest ZT value recorded was around 2.8 at 773K in a n-type single crystal of the material [11].

**Polyaniline (PANI):** Polyaniline is among the most well-researched thermoelectric materials because of its superior stability, ease of fabrication, and variable conductivity [12]. Unlike other insulators, the material features a conjugated chain of electrons that can facilitate electron flow after doping [13]. For example, in SnSe-based flexible materials, the material performs two functions; first, it acts as an elastic matrix and facilitates electric conduction by acting as a conductive path for the electrons flowing through the matrix [12]. By doing so, it overcomes the poor processibility of the inorganic material, while at the same time retaining high efficiency through energy filtering between the polymer and the inorganic phase [14].

**Polyvinylidene Fluoride (PVDF):** PVDF is one of the best thermoplastics that has been highly valued by researchers in the manufacturing of flexible devices due to its outstanding mechanical properties, chemical stability, and high thermal stability [15]. While PVDF is naturally an insulating polymer, it has excellent film-forming characteristics and is highly flexible, making it the perfect structural substrate for introducing high-performance thermoelectrics such as SnSe [16]. Moreover, it has very low thermal conductivity, which plays an important role in lowering the overall thermal conductivity of the material, hence enhancing the ZT value [17].

## **CHAPTER 2**

### **LITERATURE REVIEW**

#### **2.1 Shi, Xiao-Lei, et al [28]**

This study reviewed synthesis and thermoelectric properties of Tin Selenide. It also had basics of thermoelectricity. Reviewing this study helped us to choose the correct method of synthesis for fabrication of SnSe which was the solvothermal methods. This study also provided us with the basic idea of the expected results for the characterization and analysis of SnSe

#### **2.2 Ju, Hyun, Dabin Park, and Jooheon Kim [20]**

In this study, thin films were synthesized using the drop-casting method. It also contains methods to optimize the power factor and electrical performance of the thin films. Reviewing this study helped us to choose the drop-casting synthesis method over other thin films fabrication methods due to its advantages. Also, this study helped up to choose PVDF as the matrix material and PANI as the conducting polymer due to their favourable properties.

#### **2.3 Research Gaps**

The first cited study [28] had a detailed review of thermoelectric properties of SnSe but the study had no mentions of nanocomposites of SnSe or thin films. Although the second study [20] did have content covering the fabrication and analysis of polymer-based thin films, the idea of using SnSe with the two polymers PVDF and PANI in a thin film form is novel.

## CHAPTER 3

### EXPERIMENTAL SECTION

#### 3.1 SnSe

SnSe was prepared using the solvothermal method [21]. Solvothermal method uses nonaqueous solutions instead of water and the temperature involved in this process is relatively high [22,23]. Solvothermal method was used because SnSe crystals having favorable properties for the optimization of ZT can be synthesized using this method. Different solvents can be chosen for tuning different properties of SnSe crystals like vacancy concentration [21,24], crystalline design [21], solubility breakthrough [24,25,26] and local lattice imperfections [24,25,26]. All these properties contribute towards a higher value of ZT by increasing the Power factor while lowering the thermal conductivity.

##### 6 3.1.1 Precursors and Reagents

The following precursors and reagents were used in the solvothermal synthesis of SnSe [21],

Ethylene Glycol (EG) that is  $C_2H_6O_2$  was used as the solvent. Apart from being the solvent EG also acted like a reducing agent.

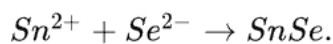
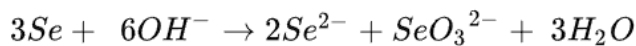
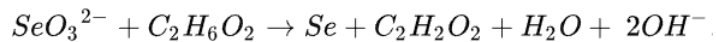
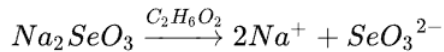
Stannous Chloride di-hydrate that is  $SnCl_2 \cdot 2H_2O$  was used as the source of  $Sn^{2+}$  ions.

Sodium Selenite that is  $Na_2SeO_3$  was used as the source of  $Se^{2-}$  ions.

Sodium Hydroxide that is NaOH was used to maintain the pH balance.

### 3.1.2 Solvothermal Synthesis of SnSe

The reactions involved in the solvothermal synthesis of SnSe are as follows [21],



The steps employed along with the stoichiometric amounts of the precursors used are as follows [21],

- 3.1g Sodium Selenite and 2.71g Stannous Chloride were dissolved in 20mL Ethylene Glycol with 2-3mL Sodium Hydroxide solution.
- This solution was stirred for around 15 minutes.
- Then this solution was kept in a Teflon-lined stainless-steel autoclave at 503K for 36h.
- Then this solution was centrifuged and the supernatant was collected.
- This supernatant was then washed with water and ethanol multiple times.
- After drying the supernatant in an oven for 12h at 333K, the Tin Selenide powder was collected.

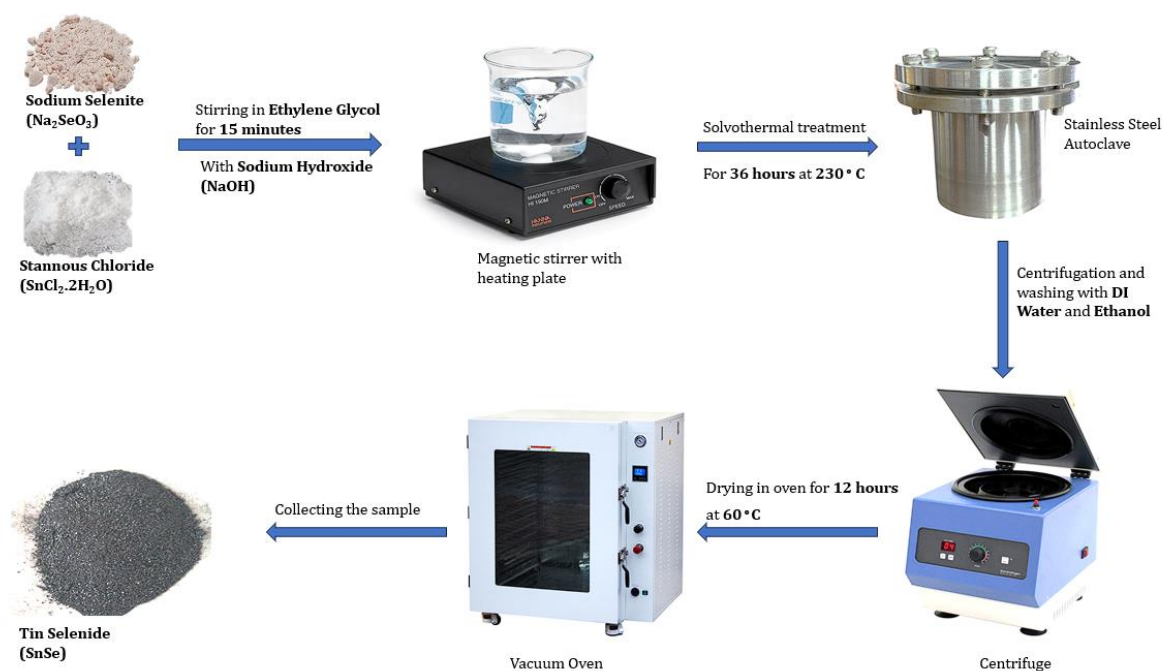


**Figure: Schematic of SnSe synthesis using solvothermal method**

### 3.2 Thin Films

The thin films were made using the drop-casting method. Drop-casting is an easily performed solution-based deposition process used for preparing thin film samples by depositing a volatile solution or suspension on a fixed substrate [18]. Spreading occurs due to gravity and capillary forces, while evaporation of the solvent leads to the formation of a thin layer of solid material on the substrate [19]. This procedure involves no special equipment under high vacuum and is easily scalable, thus offering quick prototyping [19]. Thickness of the film can be controlled through varying the solution concentrations or repeating the dropping process. It uses near-perfect atom economy and produces zero waste material, resulting in its economic efficiency [18].

7

### 3.2.1 Precursors and Reagents

The following precursors and reagents were used in the drop-casting method for the synthesis of thin films [20].

Tin Selenide (SnSe) was used as the functional thermoelectric filler.

Polyaniline (PANI) was used as the conducting polymer additive.

Polyvinylidene Fluoride (PVDF) was used as the polymer host matrix and the binder.

Dimethylformamide (DMF) is a polar aprotic solvent and was used for the following reasons,

- **Superior Polymer Solvent:** DMF stands out as an exceptional solvent for both PVDF and PANI owing to the high compatibility between DMF and PVDF's Hansen solubility parameters, making dissolutions fast and homogenous.
- **Favorable Boiling Point for Moderate Drying:** The boiling point of DMF is at 153°C. This ensures that DMF can be completely evaporated and the film dried using easily accessible hot plates within the fume hood without having much DMF trapped within the polymer structure.
- **Low Viscosity:** DMF has low viscosity, thus helping with evenly dispersing dense inorganic materials in the liquid state before casting.

Dimethyl Sulfoxide (DMSO) is also a strong polar aprotic solvent and was used for the following reasons,

- **Slow Nucleation:** Since DMSO has a higher boiling temperature of 189°C, it will take considerably more time for it to evaporate from the droplets cast on the surface. Hence, the rate of nucleation of the composite will be slower, resulting in better alignment of the polymer chains and SnSe fillers, which results in lesser defects within the crystal lattice.
- **Low Toxicity Profile:** As against DMF, DMSO shows very low toxicity levels.

### 3.2.2 Drop-Casting synthesis of Thin Films

Two different samples of thin films were synthesized with different concentration ratios of the precursors.

The steps employed along with the stoichiometric amounts of the precursors used are as follows [20],

Sample 'A' with concentration ratio 60:25:15 for PVDF, PANI and SnSe respectively.

- 600mg of PVDF was dissolved in 10mL of DMF at 70°C with continuous stirring for 5 hours.
- 250mg of PANI was dissolved in 5mL of DMF, 0.5mL of 10% DMSO was also added to the solution. Subsequent sonication for 30 minutes and stirring for 1 hour was also conducted for the same.
- 150mg of SnSe was dissolved in 5mL DMF and the solution was sonicated for 30 minutes.
- The PANI solution was added dropwise to the PVDF solution with subsequent stirring for 1.5 hours.
- In the thus formed solution, the SnSe solution was slowly added with stirring for 2 hours.
- The final formed solution was sonicated for 30 minutes.
- This final solution was drop-casted over a glass substrate using a micropipette.
- The drop-casted solution was dried overnight at 80°C and flexible thin films were obtained.

Sample 'B' with concentration ratio 60:20:20 for PVDF, PANI and SnSe respectively.

- 600mg of PVDF was dissolved in 7mL of DMF at 70°C with continuous stirring for 5 hours.
- 200mg of PANI was dissolved in 5mL of DMF, 0.5mL of 10% DMSO was also added to the solution. Subsequent sonication for 30 minutes and stirring for 1 hour was also conducted for the same.

- 200mg of SnSe was dissolved in 5mL DMF and the solution was sonicated for 30 minutes.
- The PANI solution was added dropwise to the PVDF solution with subsequent stirring for 1.5 hours.
- In the thus formed solution, the SnSe solution was slowly added with stirring for 2 hours.
- The final formed solution was sonicated for 30 minutes.
- This final solution was drop-casted over a glass substrate using a micropipette.
- The drop-casted solution was dried overnight at 80°C and flexible thin films were obtained.

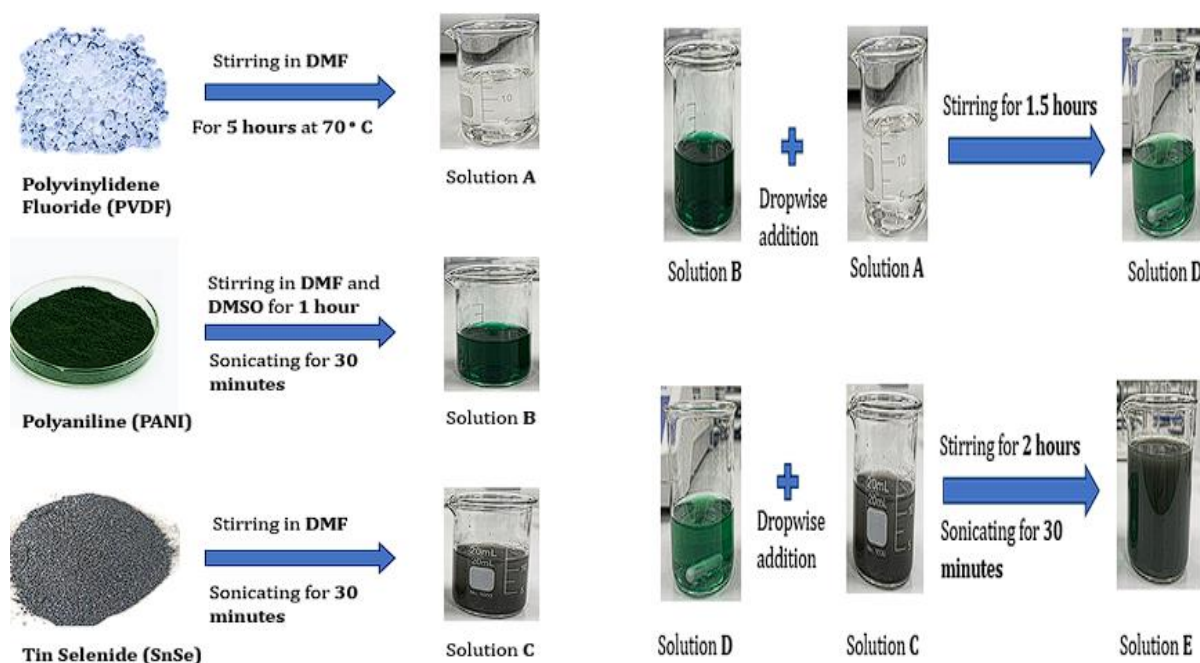


**Figure: Schematic of Solution Preparation for Drop-Casting**

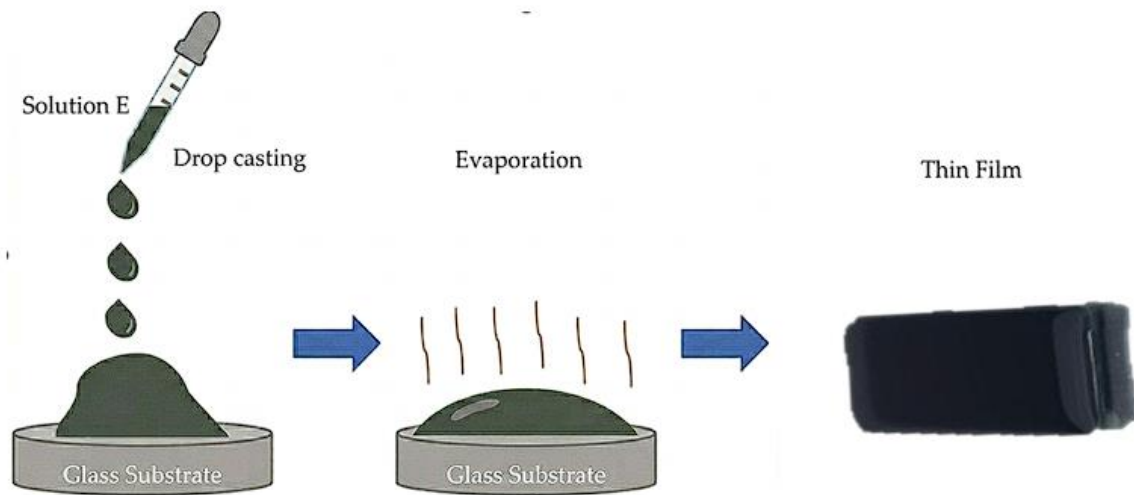


**Figure: Schematic of Drop-Casting Synthesis of Thin Films**

## CHAPTER 4

### CHARACTERIZATION AND ANALYSIS

#### **4.1 Characterization Techniques**

The crystallographic characterization is done by Xray Diffraction of Tin Selenide using  $K\alpha$ Cu wavelength. The crystallite size of SnSe is calculated using Debye-Scherrer formula is around 115 nm. The W-H plot of SnSe is constructed to calculate the crystallite size of sample which is approximately 120 nm. The bond stretching of SnSe is analysed using Fourier transform infrared microscopy. The electrical performance is assessed via the I-V characteristic curve. The thermal stability is studied via the Electrical conductivity vs Temperature curve. The thermoelectric performance is analysed using the Seebeck Coefficient vs Temperature curve.

For analysis of the thin films Xray Diffraction is conducted using  $K\alpha$ Cu wavelength. The electrical performance is assessed via the I-V Characteristic curve. The thermal stability is studied via the Electrical Conductivity vs Temperature curve.

## 4.2 Result and discussion

### XRD Analysis of SnSe

Xray pattern in figure shown explains about the crystal analysis of SnSe crystal. The SnSe crystal exhibits orthorhombic crystal structure with space group correspond to Pnma.

The peaks in the XRD pattern at  $30.4^\circ$ ,  $30.9^\circ$ ,  $49.6^\circ$ ,  $51.7^\circ$ ,  $64.7^\circ$ ,  $68.9^\circ$ ,  $77.4^\circ$  correspond to (111), (400), (511), (402), (203), (213), (901) diffraction planes of SnSe. The lattice parameters  $a(\text{\AA})$ ,  $b(\text{\AA})$  and  $c(\text{\AA})$  are calculated to be 11.37, 4.186, 4.44 respectively. For d-spacing calculation we use the Bragg' law formula.

$$2d\sin(\theta) = n\lambda$$

Where the  $\theta$  is Bragg's angle and  $\lambda$  is the wavelength of the X-ray

The d-spacing was calculated to be  $2.8853(\text{\AA})$  corresponding to (400) plane

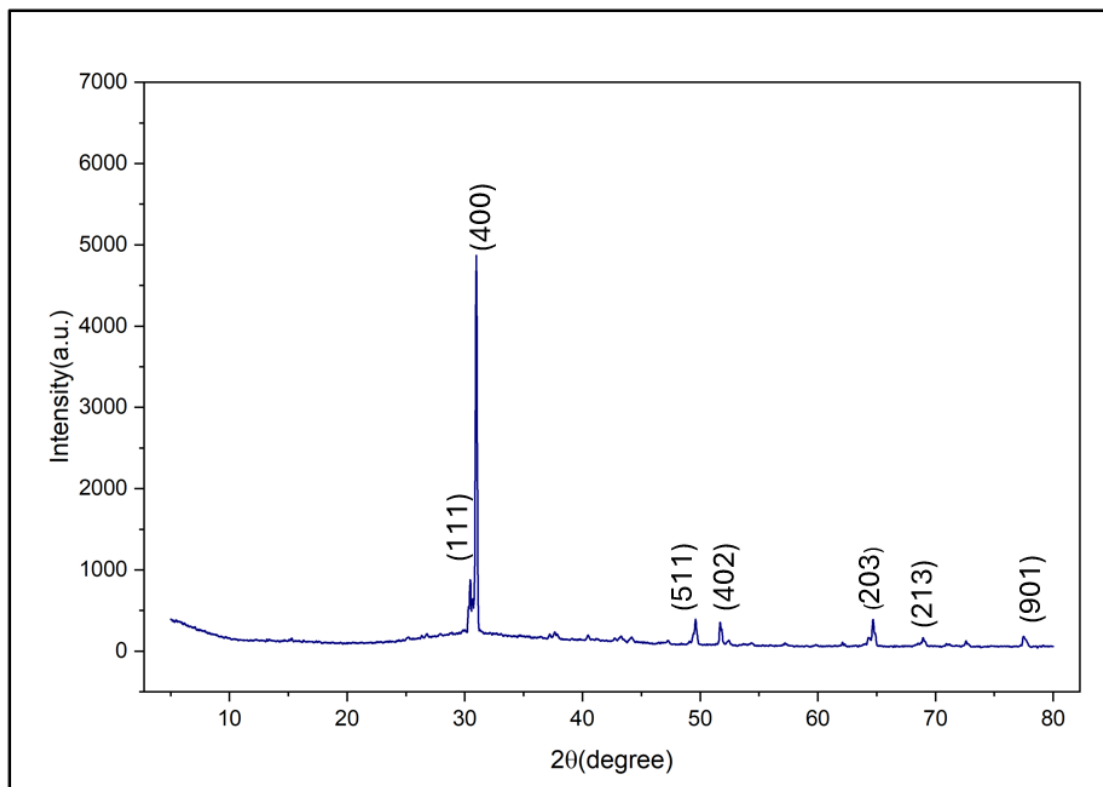


Figure: XRD pattern

To calculate the crystallite size of obtained material we use Debye-Scherrer's formula.

$$D = \frac{K\lambda}{\beta \cos\theta}, \text{ where}$$

$D$  = crystallite size,

$K$  = shape factor,

$\beta$  = FWHM,

$\lambda$  = wavelength of  $\text{CuK}\alpha$ .

$\theta$  = Bragg's angle.

The calculated value of crystallite size is 114.9nm.

For further analysis of macrostrain present in the orthogonal structure of SnSe we use Willum-Hall plot shown in figure. The formula associated W-H plot is

- $\beta_{\text{total}} = \beta_{\text{crystalline size}} + \beta_{\text{macrostrain}}$
- $\beta_{\text{total}} = \frac{k\lambda}{D \cos\theta} + 4\epsilon \tan\theta$

where,  $\beta$  is FWHM,  $\epsilon$  is the slope of the W-H plot

The calculated crystallite size is 120.6nm with intercept of 0.0012.

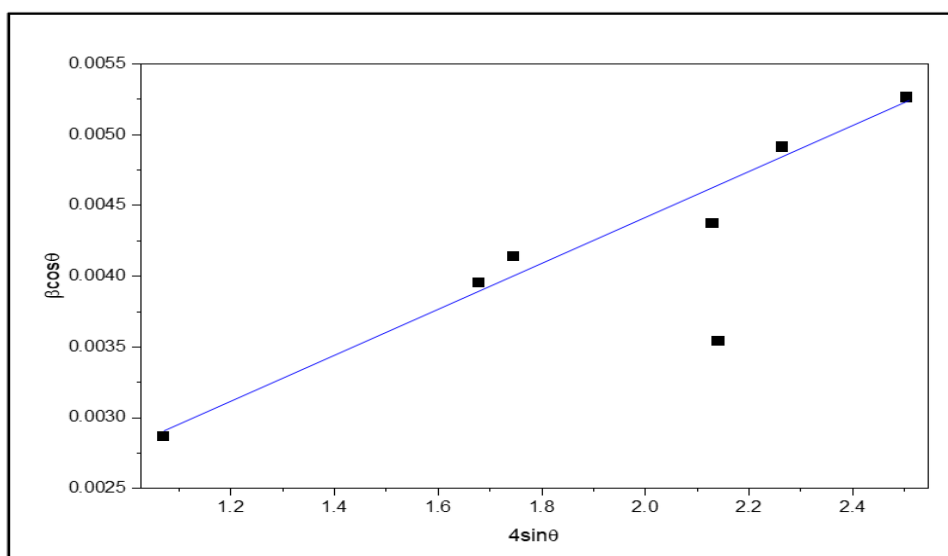


Figure: W-H plot of Xrd pattern

## FTIR Analysis of SnSe

Fourier Transform Infrared spectroscopy is the characterization technique used to observe the vibrational and rotational energy of a compound. It is used to analyze about the stretching and bending of bonds associated within the compound. The graph is plotted between the transmitted radiation with respect to the wavelength ( $\text{cm}^{-1}$ ). The range of wavelength of FTIR is from 4000 to 400  $\text{cm}^{-1}$ .

From ( $3550 \text{ cm}^{-1} - 3300 \text{ cm}^{-1}$ ) it shows the O-H stretching vibrations due to absorbed water.

Peak at  $1636 \text{ cm}^{-1}$  due to H-OH bending due to moisture (during washing) remains in SnSe.

Peak at  $827 \text{ cm}^{-1}$  explains the Se-O OR Sn-O stretching due to surface oxygen.

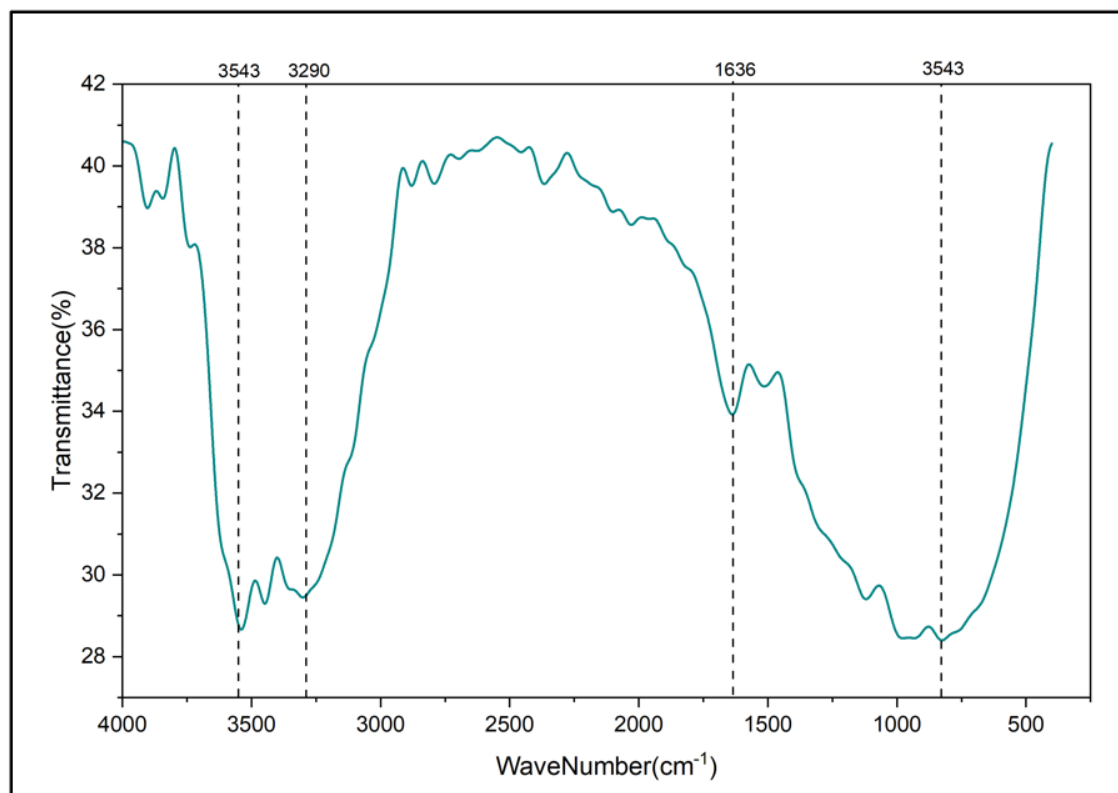


**Figure: FTIR spectra**

## I-V Characteristics of SnSe

The current-voltage (I-V) curve is a key electrical parameter that is used for characterizing charge transport properties of a material or compound. The curve shows the dependence of voltage and the current flowing through it. Here, we find that there is a square pellet of SnSe with terminal points labelled A, B, C, and D, which correspond to the curves as  $V_{ab}$ ,  $V_{bc}$ ,  $V_{cd}$ , and  $V_{da}$ . Here, the test has been conducted with current sweeping from  $-1.0$  mA to  $+1.0$  mA.

- The resistance across  $V_{ab}$  is  $734.1\Omega$  which shows ohmic nature.
- The resistance across  $V_{bc}$  is  $877.3\Omega$  which shows saturated ohmic nature.
- The resistance across  $V_{cd}$  is  $1238.9\Omega$  which shows deviated ohmic nature.
- The resistance across  $V_{da}$  is  $1059.1\Omega$  which shows ohmic nature.

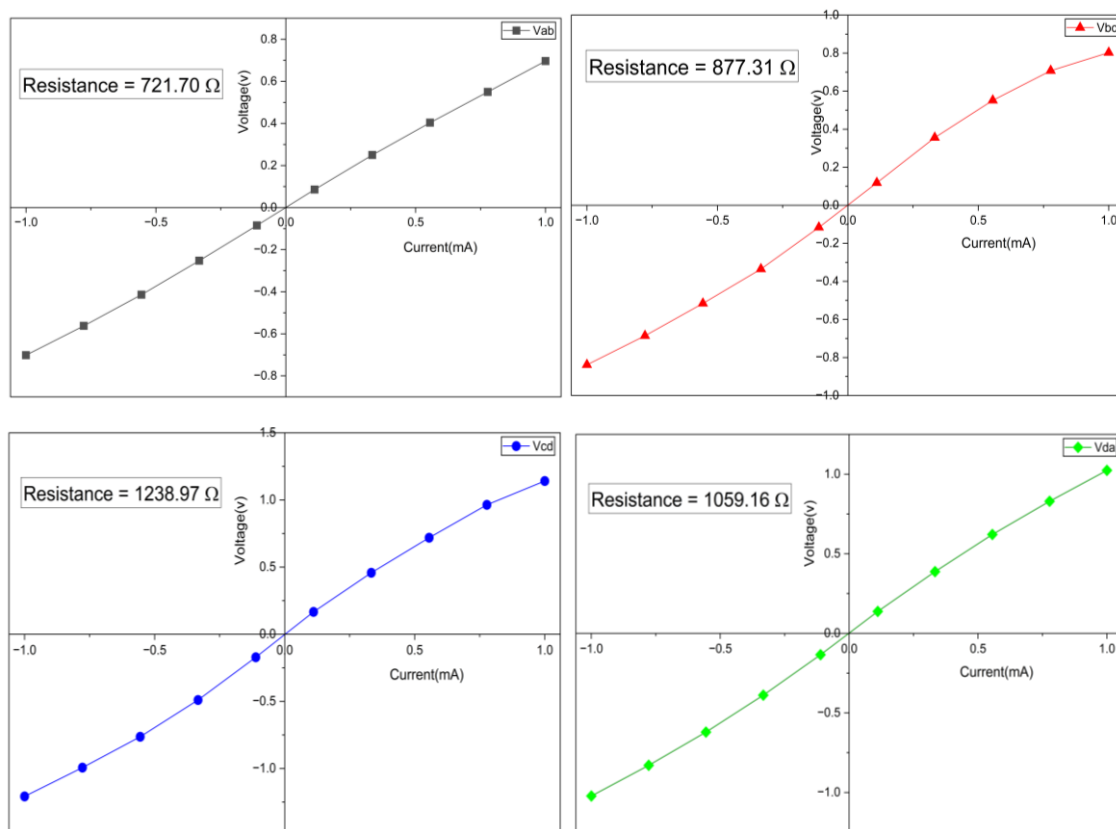


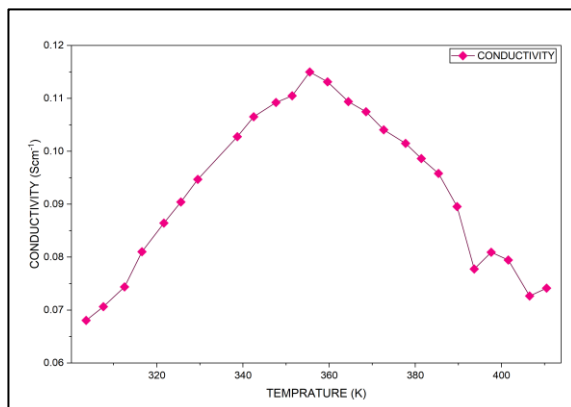
Figure: I-V characteristics

## Electrical Conductivity vs Temperature curve of SnSe

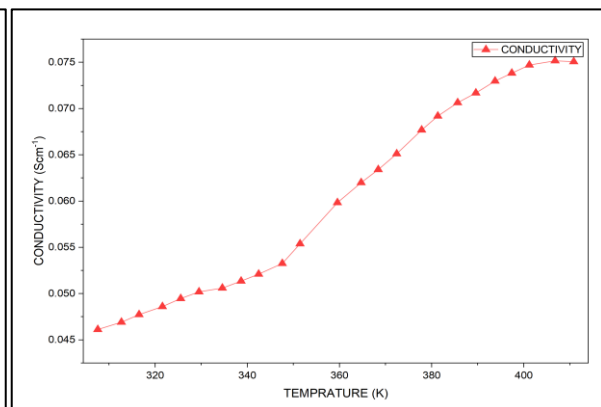
Electric conductivity is an indication of how well the current can flow through the SnSe pellet. Conductivity varies greatly with temperature. Temperature dependence of the electric conductivity ( $\sigma$ ) of the prepared bulk SnSe pellet was studied for two successive thermal cycles between 305K and 410K.

### Run 1

- In heating cycle (1a) the conductivity begins from  $\sim 0.068 \text{ Scm}^{-1}$  at 305K.
- In figure (1a) conductivity rises linearly until it reaches a sharp peak of  $\sim 0.115 \text{ S cm}^{-1}$  at 355K. Then conductivity subsequently drops drastically to  $\sim 0.074 \text{ Scm}^{-1}$  at 410K.
- In cooling cycle (1b) on being cooled from 410K, the compound doesn't follow its heating curve backwards.
- The curve shows a consistent decrease in conductivity, acting as a typical semiconductor through the whole cooling process and finally settling to a new base value  $\sim 0.046 \text{ Scm}^{-1}$  at 305K.



1(a)

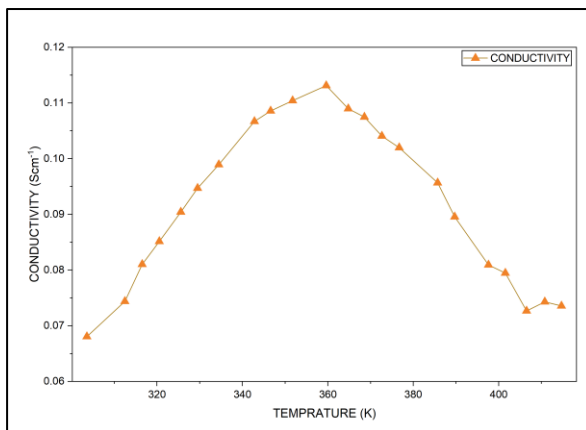


1(b)

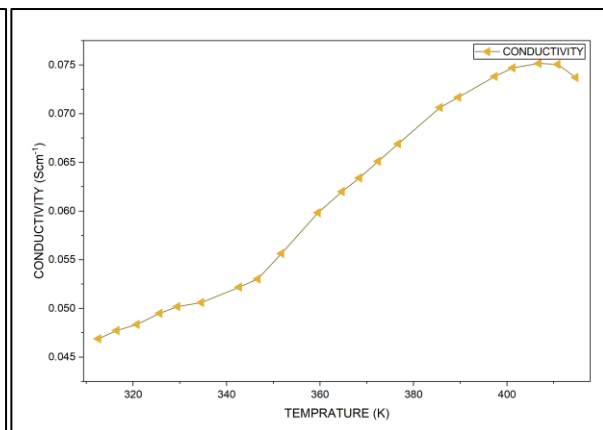
**Figure: Conductivity vs Temperature**

## Run 2

- In heating cycle (2a) the substance behaves similarly as compared to the first heat cycle.
- Here the conductivity rises from its lower level to a maximum value of  $\sim 0.113 \text{ Scm}^{-1}$  at 360K. Further it drops to  $\sim 0.073 \text{ Scm}^{-1}$  at 405K.
- In cooling cycle (2b) Conductivity path exactly corresponds to the first cooling curve.
- The value of conductivity declined to  $\sim 0.047 \text{ Scm}^{-1}$  at 310K.



2(a)



2(b)

**Figure: Conductivity vs Temperature**

Therefore, after comparing both the tests we can conclude that heating the SnSe pallet up to 410K does not change its structure permanently.

## Seebeck Coefficient vs Temperature curve of SnSe

The Seebeck coefficient (S) is an intrinsic characteristic of electrical conduction, which measures the amplitude of a change in voltage created by a temperature gradient in SnSe pellet.

The curve represents the value of Seebeck coefficient at different temperature starting from 305K to 410K.

### RUN 1

- The Seebeck coefficient is always positive across the full temperature range 305K to 410K, and ranges from  $+140 \mu\text{V K}^{-1}$  to  $+165 \mu\text{V K}^{-1}$ . It is thus proven that the bulk SnSe is p-type semiconductor.
- The calculated slope is found out to be  $-1.847 \times 10^{-4} \text{ V K}^{-1}$ . The negative sign suggests an increasing trend ( $dS/dT < 0$ ) due to the gradual thermally-driven increase in the number of majority carriers.

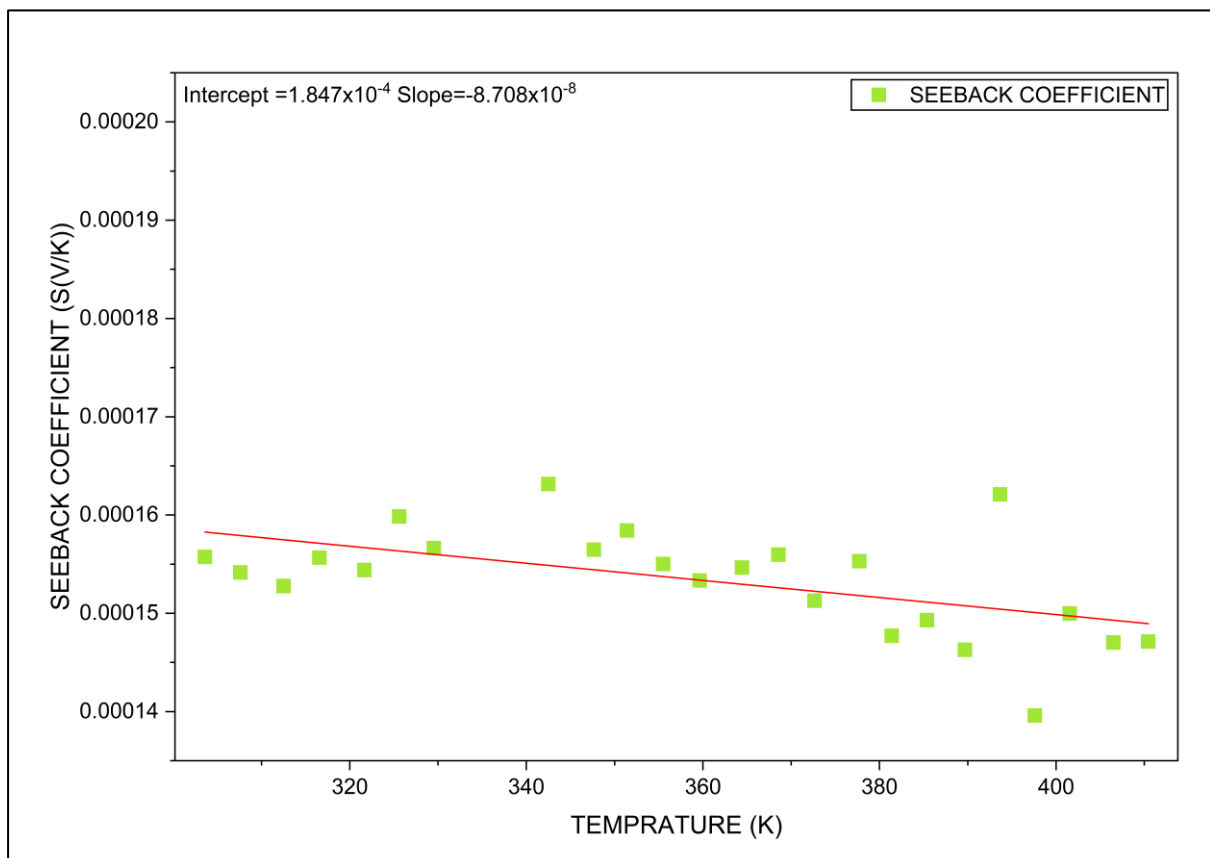
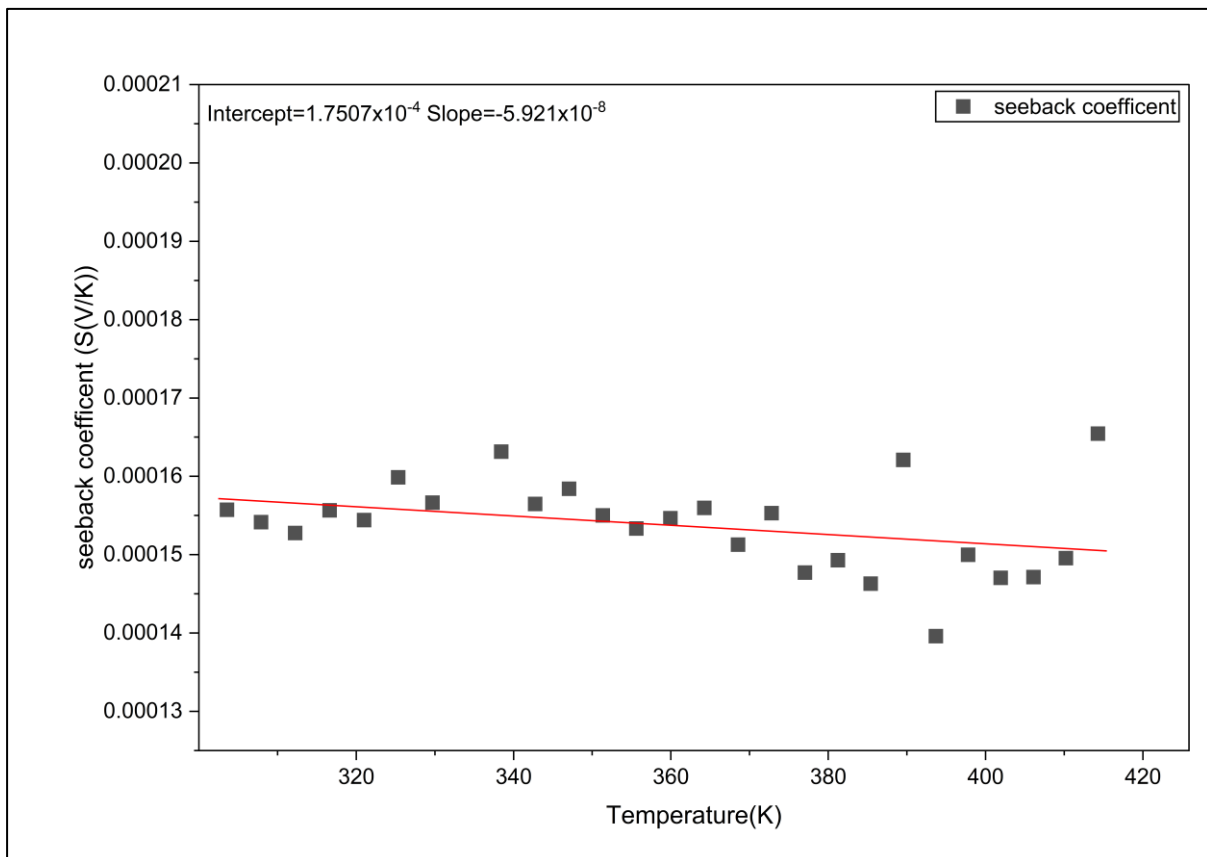


Figure: Seebeck coefficient vs Temperature

## RUN 2

- The curve is similar to the first one because the sign stays positive for all temperatures, indicating that there was neither thermal instability nor reversal of the polarity of majority carriers. The readings fall between the same bounds, namely  $+140 \mu\text{V K}^{-1}$  and  $+165 \mu\text{V K}^{-1}$ .
- For the second cycle, the slope obtained is  $1.750 \times 10^{-4}$ . This shows a slight reduction in the slope of the graph compared to that obtained for the first cycle because of the structural stabilization caused by the previous cycle of heating.



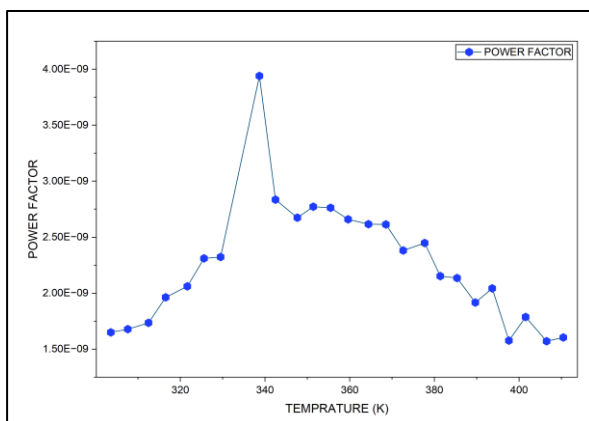
**Figure: Seebeck coefficient vs Temperature**

## Power factor vs Temperature curve of SnSe

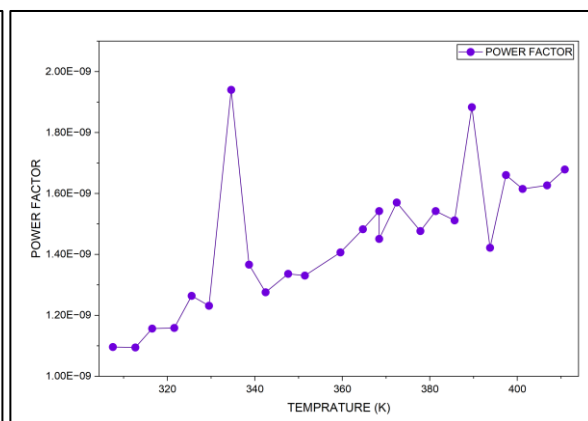
In order to link these two independent measurements of electrical conductivity ( $\sigma$ ) and Seebeck coefficient ( $S$ ), it is essential to evaluate the temperature-dependent thermoelectric power factor (PF). The power factor can be regarded as the ultimate criterion to measure the electrical quality of a material and its ability to generate electricity.

### Run 1

- During the heating cycle (1a) the temperature increases from 300K, the power factor increases continuously from its starting value  $1.65 \times 10^{-9} \text{Wcm}^{-1}\text{K}^{-2}$ . The starting window for this increase corresponds to the combined effect of increasing electrical conductivity and maintained Seebeck coefficient.
- The calculated slope is found out to be  $2.746 \times 10^{-9} \text{Wcm}^{-1}\text{K}^{-2}$  which gives the overall output power factor value starting from range 300K to 420K during heating cycle.
- The cooling plot (1b) shows no such broad region for 340K to 360K, but it falls to a lower operating power and settles around  $1.10 \times 10^{-9} \text{ c}$ . This confirms that the highly conducting state observed during heating is kinetically barred from reforming due to structural relaxation delays.
- Here the slope is calculated to be  $-6.663 \times 10^{-10} \text{Wcm}^{-1}\text{K}^{-2}$ , due to reduced thermal energy and fewer charge carrier excitations.



1(a)

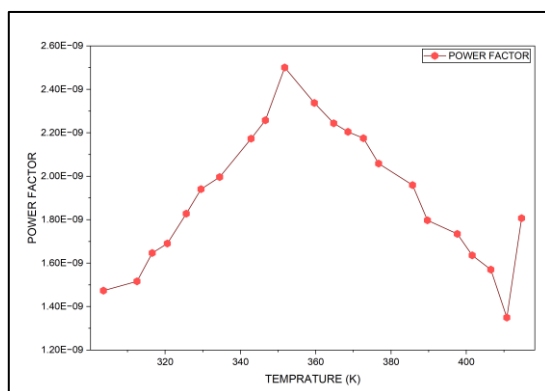


1(b)

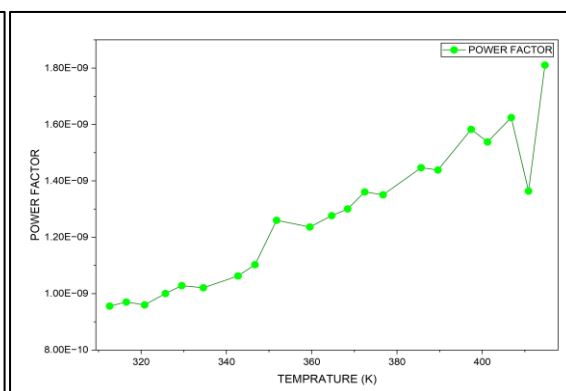
**Figure: Power factor vs Temperature**

## Run 2

- Now the heating cycle (2a) shows raising PF value from 305K to 355K then it drops till temperature reaches 410K. This causes due increase of carrier mobility at low temperature range and increase in carrier scattering (increases resistance) at high temperature.
- The overall slope of heating curve is  $1.99 \times 10^{-9} \text{ Wcm}^{-1}\text{K}^{-2}$ . This value explains the significant stabilization of the initial thermal cycle permanently altered or eliminated highly unstable, shallow defect states, hence the overall value increases.
- As soon as the pellet is subjected to a temperature of 410K, the increased thermal energy leads to an adjustment in the lattice structure, thereby relieving mechanical stresses built up in the grain boundary structure. As soon as the cooling cycle (2b) is started, the rate of cooling exceeds that of the relaxation process. It justifies the negative slope  $-1.324 \times 10^{-9} \text{ Wcm}^{-1}\text{K}^{-2}$ . This negative slope confirms that the cooling cycle consistently operates as a single-phase, where the power factor decays monotonically as charge carriers freeze out with decreasing thermal energy and carrier mobility.



2(a)



2(b)

**Figure: Power factor vs Temperature**

## TGA-DSC of SnSe

Thermogravimetric analysis and differential scanning calorimetry together (TGA-DSC) form a very strong thermos-analytical tool used for analysing the thermal stability, composition integrity, and thermodynamic phase transitions of functional materials. TGA analyses the variation in the physical mass of the sample with respect to change in temperature/time by determining processes such as evaporation, sublimation, decomposition, or oxidation kinetics.

- The curve of TGA stays almost constant until a temperature close to 800°C without any substantial weight loss. This suggests that the material used is a stable compound with no surface contamination and moisture absorption.
- After crossing 800°C the sample loses 26.63% weight.

The DSC curve tracks structural phase modifications via energy exchanges. The upward peaks represent exothermic reactions.

- At temperature 638.17°C, the enthalpy Changes by 1490.61mJ.
- At room temperature, it possesses a highly distorted orthorhombic structure with a Pnma space group. On heating, it transitions into a more symmetric Cmcm space group.

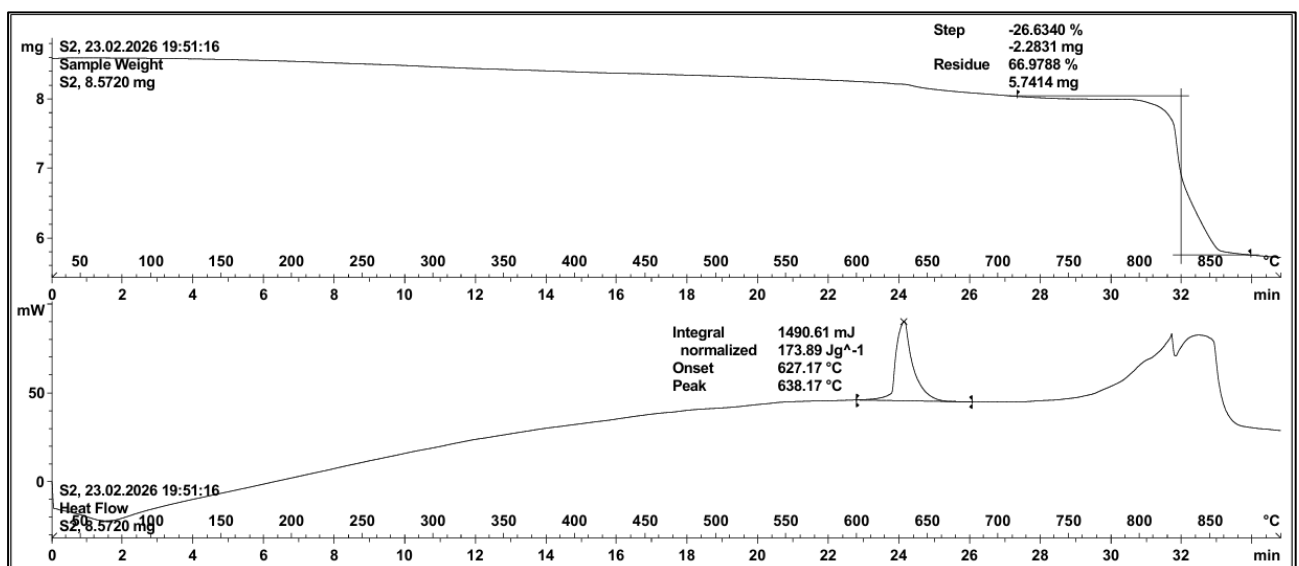
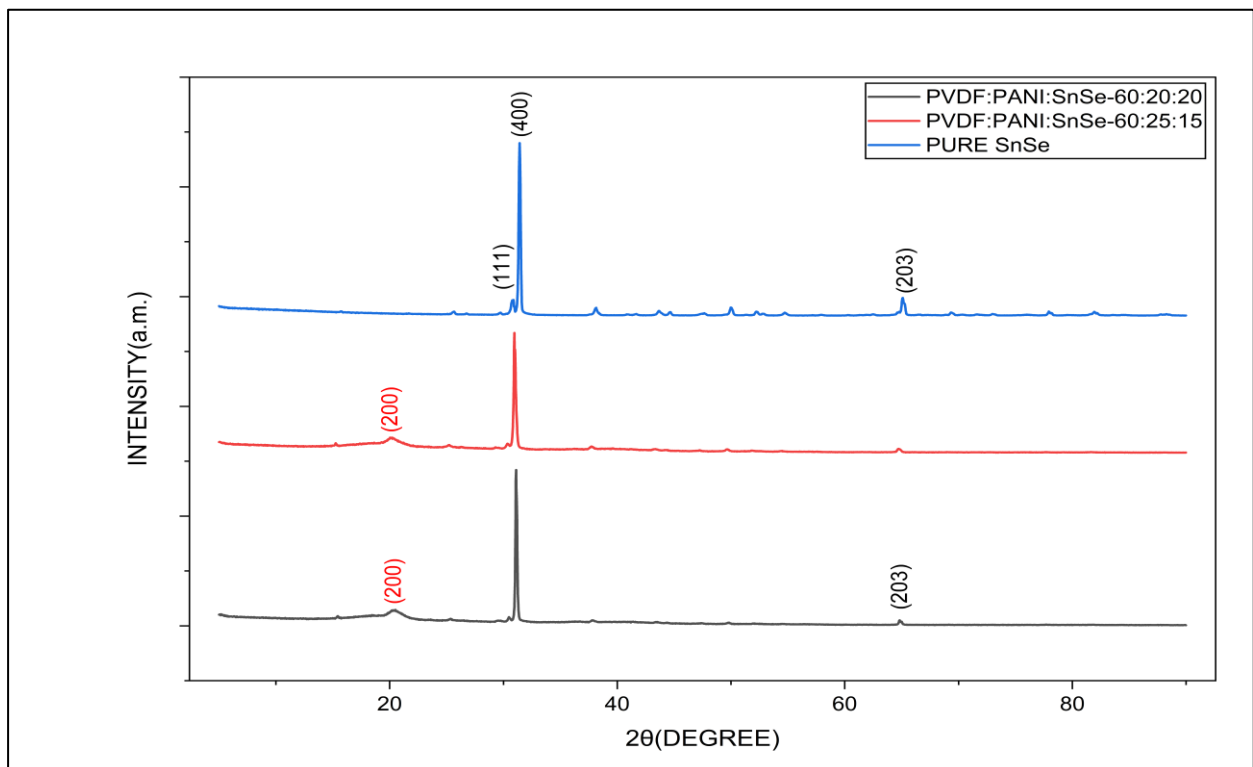


Figure: TGA-DSC Curve

## XRD Analysis of Thin Films

The XRD studies of the thin films showed differences in compositions with peak shifts, which are solely dependent on the different mixing proportions of each component. The XRD patterns have shown that the exact crystallographic planes of the crystalline SnSe along with the signature of the polymer matrix were successfully recognized. It is important to note that the formation of narrow diffraction peaks has proven the high degree of crystallinity of SnSe, while the formation of broad halos indicates the amorphous and semi-crystalline nature of the host polymer matrix.

- As observed peaks at  $30.8^\circ$ ,  $31.4^\circ$  and  $64.09^\circ$  correspond to planes (111), (400) and (203) of pure SnSe
- The broad peak at  $20.4^\circ$  and a shifted peak at  $31.4^\circ$  of plane (200) explains the composition of  $\beta$ -phase PVDF and PANI.



**Figure: XRD Spectra**

## FTIR Analysis of Thin Films

FTIR spectroscopy technique has been used in the current study to evaluate the structures of PVDF, PANI and SnSe composite thin films. The FTIR spectra of the thin films show the presence of characteristic functional groups of both PVDF and PANI. It also shows the interaction of the polymer matrix with the SnSe nanoparticles.

### Sample A (PVDF:PANI:SnSe = 60:25:15)

- Peak at  $2975\text{ cm}^{-1}$  gives C–H stretching vibrations, at  $1585\text{ cm}^{-1}$  gives C=C stretching, at  $1490\text{ cm}^{-1}$  gives C-H bending/skeletal vibration in aromatic systems which explains the presence of organic compound.
- Peak at  $1397\text{ cm}^{-1}$  gives C-N stretching vibrations and  $872\text{--}827\text{ cm}^{-1}$  band of Metal–O–Metal stretching vibrations explains about the bonding due to PVDF polymer.
- Peak at  $1162\text{ cm}^{-1}$  gives C-O stretching and electron band happens due to oxidising state of PANI polymer.
- Peak at  $432\text{ cm}^{-1}$  gives Strong Metal–O stretching vibration due to presence of SnSe.

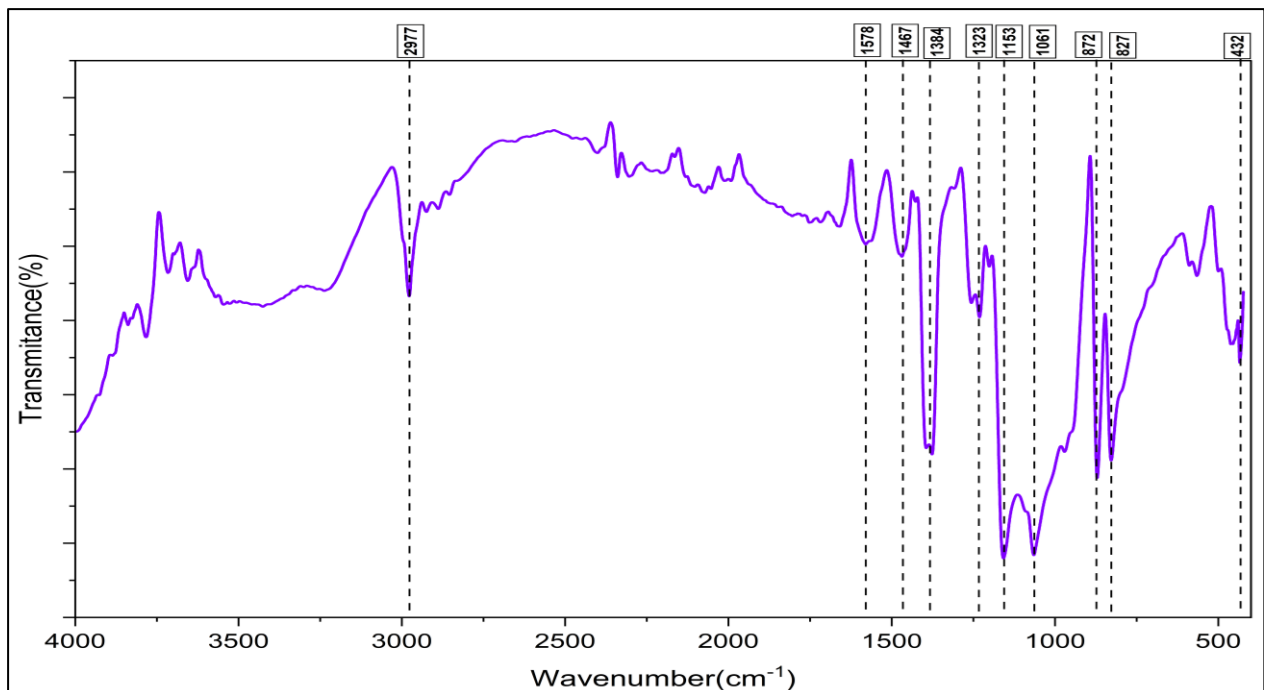
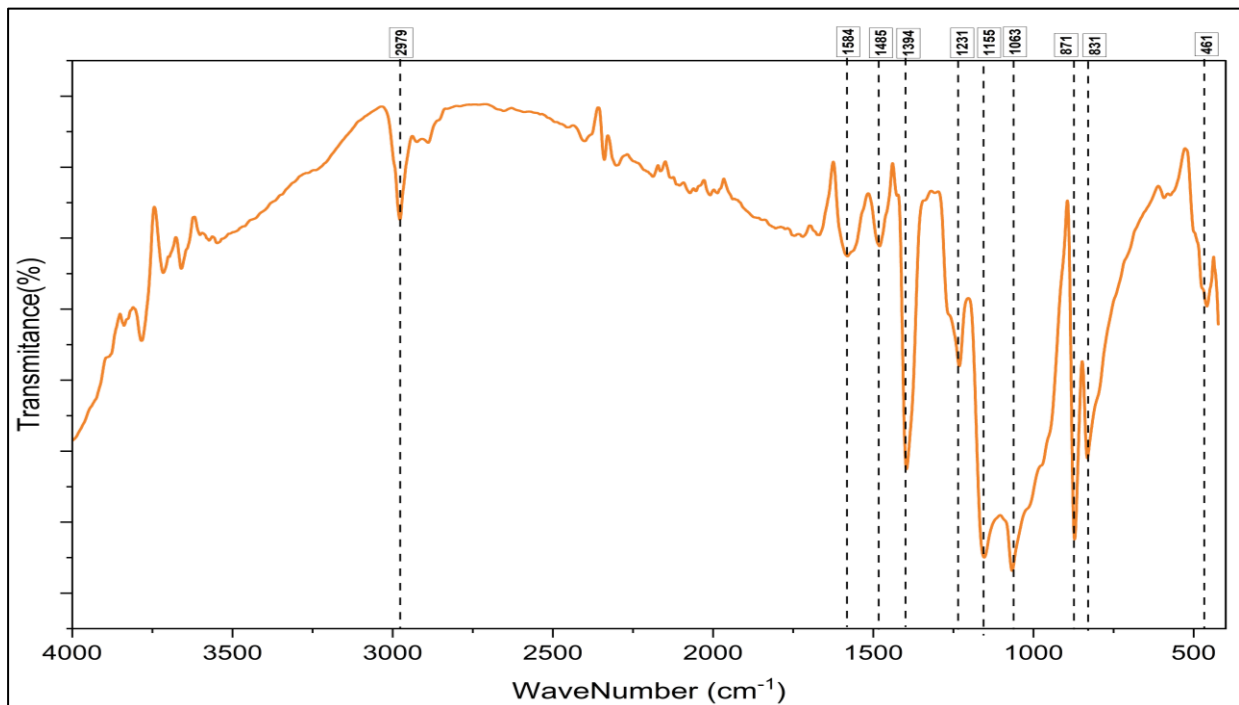


Figure: FTIR Spectra

## Sample B (PVDF:PANI:SnSe = 60:20:20)

- Similar to the previous sample but as the composition of SnSe is increased by 5% and composition of PANI is decreased by 5% it shows shifted peaks.
- The sharpness of the peak at  $831\text{cm}^{-1}$  indicates that the increased concentration of the SnSe nanoparticles works well as a good nucleating agent for the electroactive domain of the polymer matrix.
- Shifted peak at  $461\text{cm}^{-1}$  indicates high inorganic interaction due to increase in SnSe concentration.



**Figure: FTIR Spectra**

## I-V Characteristics of Thin Films.

### Sample A (PVDF:PANI:SnSe = 60:25:15)

#### Run 1

- The resistance across  $V_{ab}$  is  $11.3 \times 10^4 \Omega$  which shows perfectly ohmic nature.
- The resistance across  $V_{bc}$  is  $5.1 \times 10^4 \Omega$  which shows linear ohmic nature.
- The resistance across  $V_{cd}$  is  $5.9 \times 10^4 \Omega$  which shows symmetric non-ohmic nature.
- The resistance across  $V_{da}$  is  $9.9 \times 10^4 \Omega$  which shows non-ohmic nature. The increase in the value of current causes the strength of the electric field to rise and thus the drift velocity decreases.

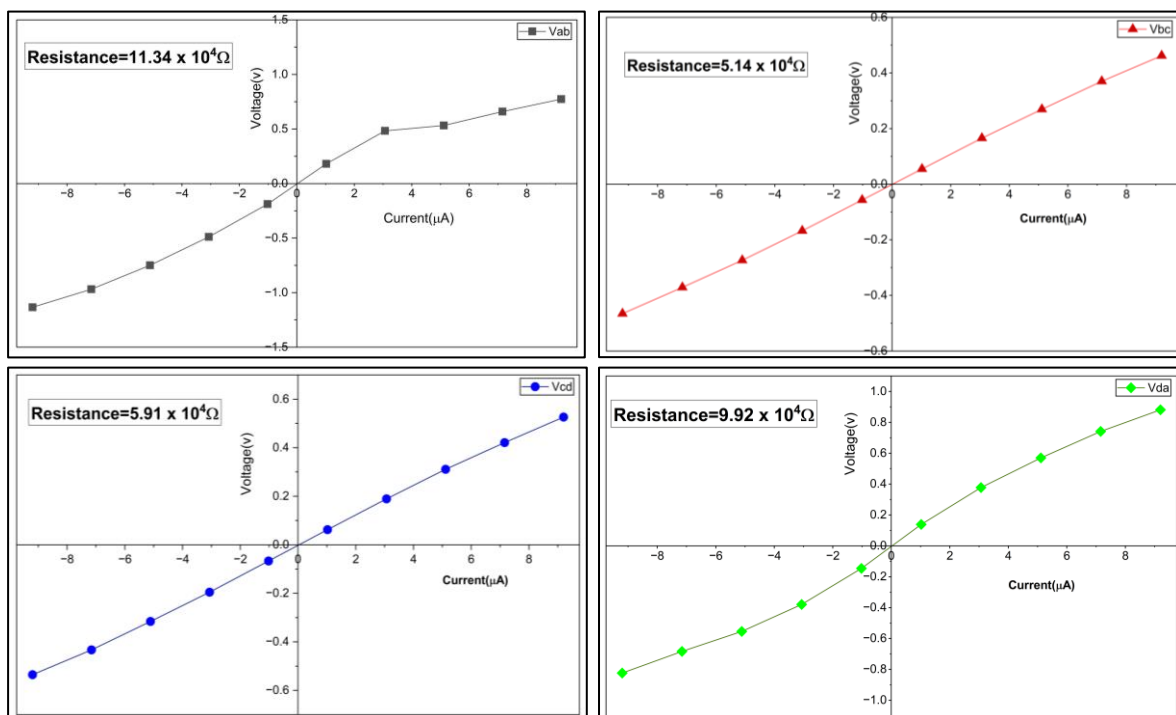
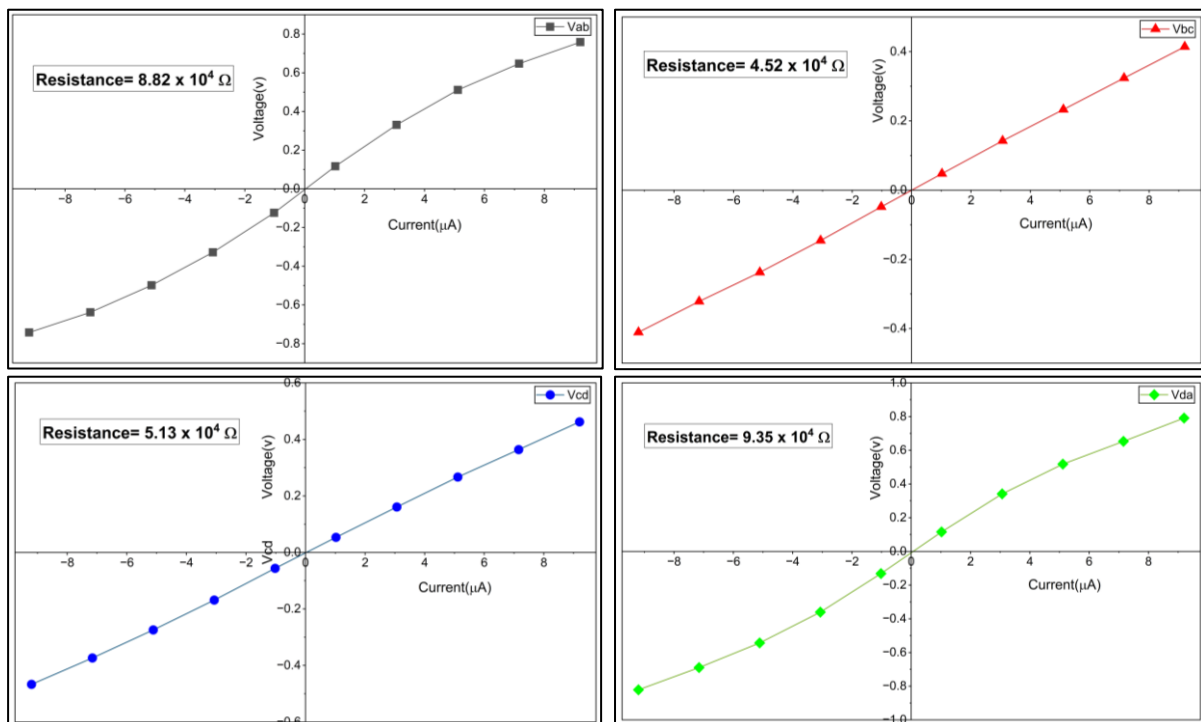


Figure: I-V Characteristics

## Run 2

- The resistance across  $V_{ab}$  is  $8.8 \times 10^4 \Omega$  which shows highly symmetric, stable sub-linear ohmic nature.
- The resistance across  $V_{bc}$  is  $4.5 \times 10^4 \Omega$  which shows ideally linear ohmic nature.
- The resistance across  $V_{cd}$  is  $5.1 \times 10^4 \Omega$  which shows perfectly linear ohmic nature.
- The resistance across  $V_{da}$  is  $9.35 \times 10^4 \Omega$  which shows symmetric non-ohmic nature.



**Figure: I-V Characteristics**

The concentration of SnSe is low and high composition of PANI increases the electrical conductivity so the resistance is low as compared to sample B.

## Sample B (PVDF:PANI:SnSe = 60:20:20)

### Run 1

- The resistance across  $V_{ab}$  is  $8 \times 10^4 \Omega$  which shows ohmic nature.
- The resistance across  $V_{bc}$  is  $6.3 \times 10^4 \Omega$  which shows ohmic nature.
- The resistance across  $V_{cd}$  is  $6.34 \times 10^4 \Omega$  which shows saturated ohmic nature.
- The resistance across  $V_{da}$  is  $7.2 \times 10^4 \Omega$  which shows non-ohmic nature.

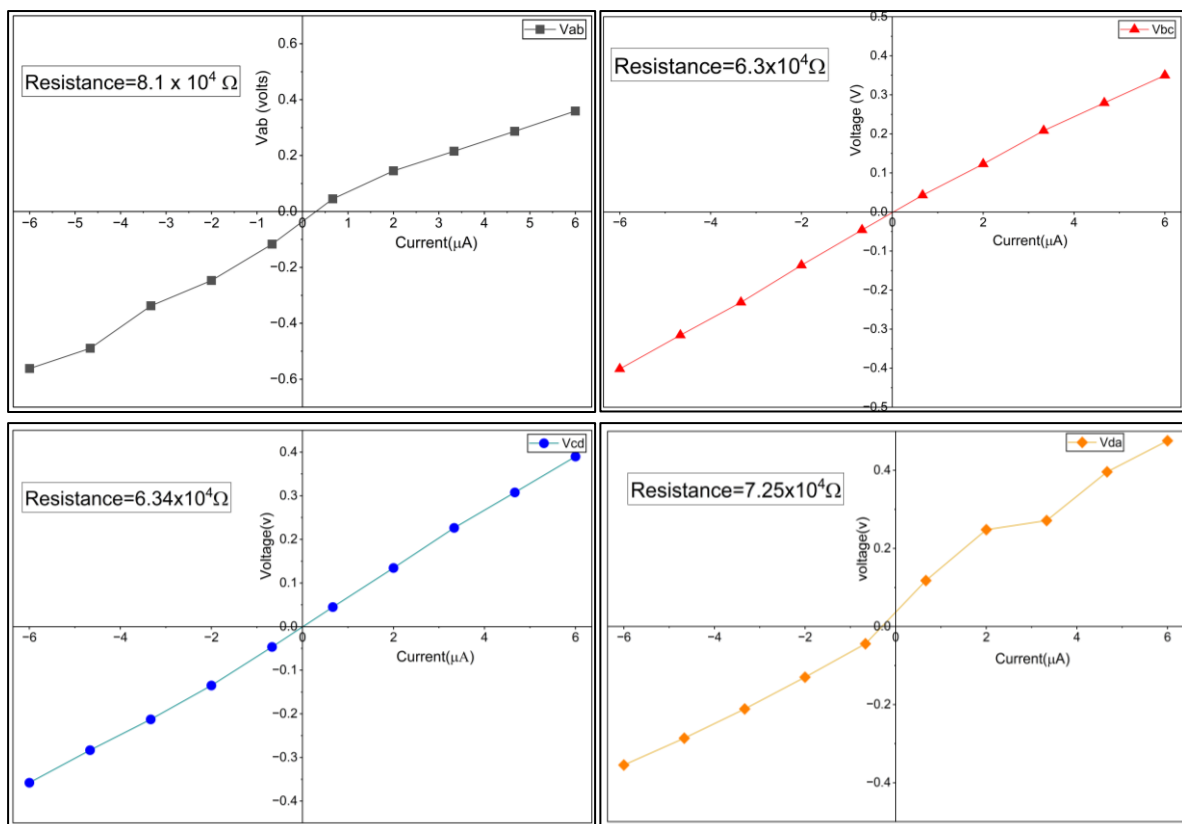


Figure: I-V Characteristics

## Run 2

- The resistance across  $V_{ab}$  is  $12.96 \times 10^4 \Omega$  which shows Linear ohmic nature.
- The resistance across  $V_{bc}$  is  $16.7 \times 10^4 \Omega$  which shows ohmic nature.
- The resistance across  $V_{cd}$  is  $25.6 \times 10^4 \Omega$  which shows asymmetric non-ohmic nature.
- The resistance across  $V_{da}$  is  $22.4 \times 10^4 \Omega$  which shows non-ohmic nature.

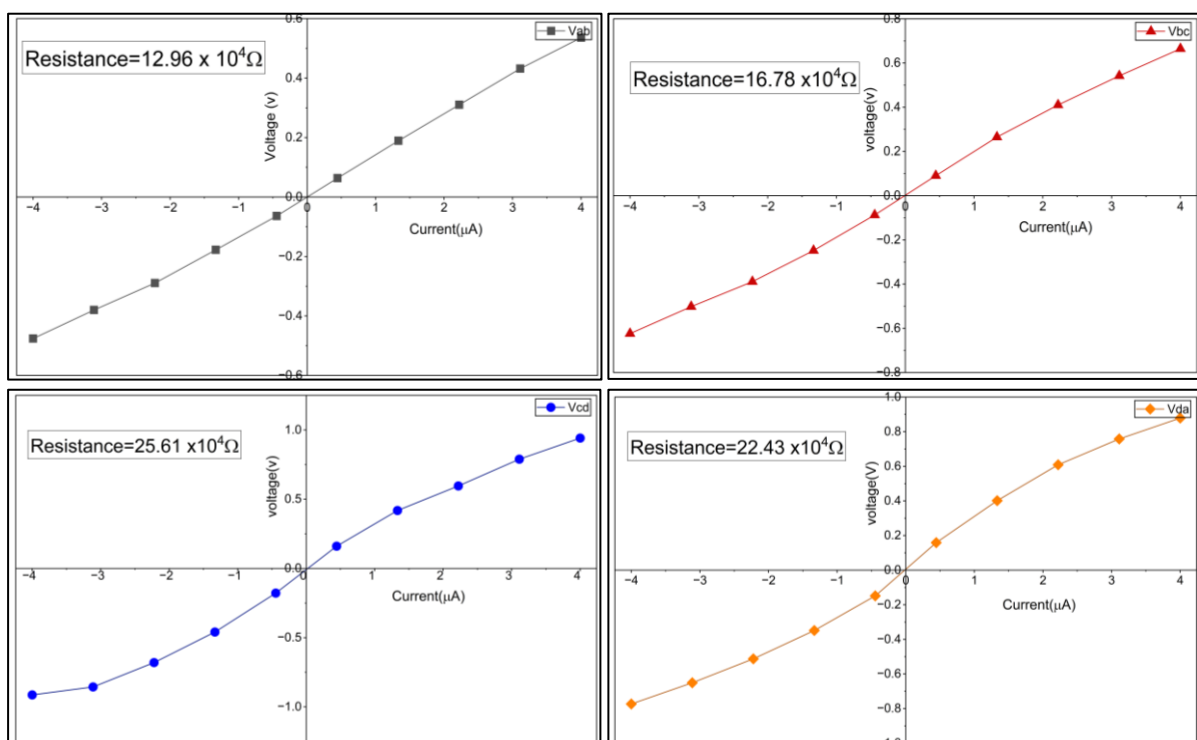


Figure: I-V Characteristics

The resistance changes between Run1 and Run2 explains about the electrical trapping of charges due to defects of thin films. This shows the dynamic electrical property of thin films.

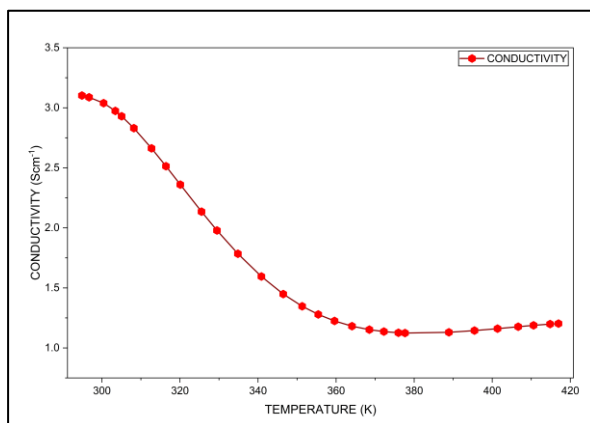
## Electrical Conductivity vs Temperature Curve of Thin Films

The conductivity curve of film provides the information about the charge carrier mobility and structural stability with change in temperature across the film.

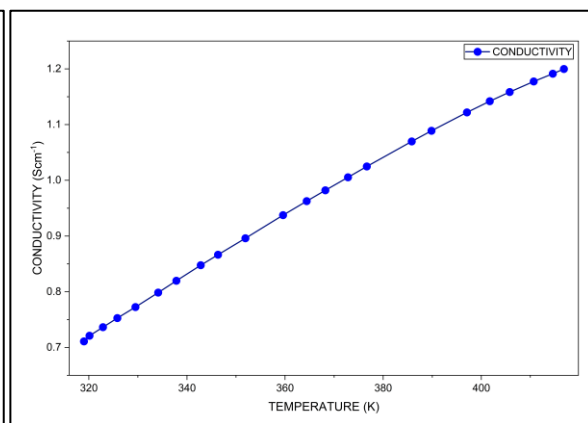
### Sample A (PVDF:PANI:SnSe = 60:25:15)

#### Run 1

- At room temperature 295K, the conductivity of the thin film attains its maximum value of  $\sim 3.1 \text{ Scm}^{-1}$ . With increasing temperatures from 295K to 376K, the conductivity progressively reduces to attain its minimum value of  $\sim 1.1 \text{ Scm}^{-1}$ .
- After 376K, the conductivity reaches a saturation state and gives the constant value of  $\sim 1.2 \text{ Scm}^{-1}$  till 418K due to thermally activated semiconducting behaviour.
- As the temperature is reduced from 418K to 320K, the curve does not follow the path of heating curve (1a) and conductivity decreases monotonically.
- The cooling curve (1b) starts at  $\sim 1.2 \text{ Scm}^{-1}$  and ends at  $\sim 0.71 \text{ Scm}^{-1}$ . The decrease in temperature T causes a decrease in thermal energy which then charge carriers transitions between the PANI chains and SnSe grains.



1(a)

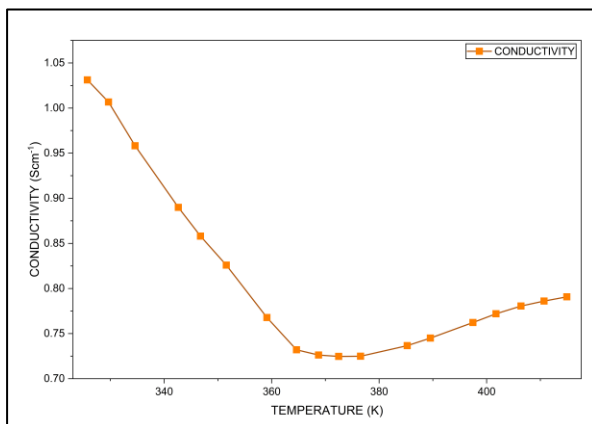


1(b)

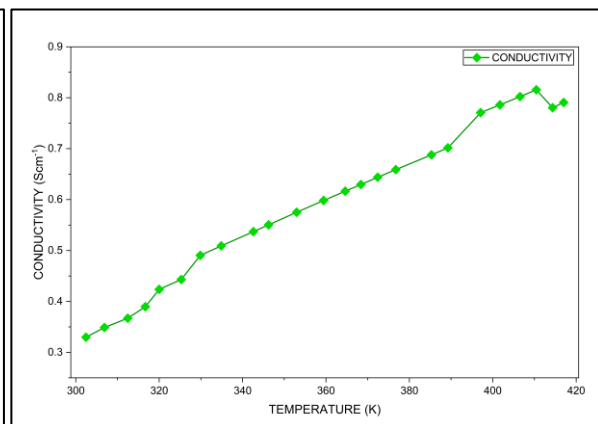
Figure: Conductivity vs Temperature

## Run 2

- The Run 2 heating cycle (2a) show similar curve as before where conductivity decrease in monotonic behaviour in the range 325K to 375K.
- The initial conductivity was  $1.03\text{Scm}^{-1}$  which further decreased to  $0.72\text{Scm}^{-1}$ . As the sample is heated PVDF material becomes mobile in certain regions, enabling the PANI and SnSe materials to align together which decrease conductivity.
- In cooling curve (2b), after being cooled from 415K to nearly room temperature at 302K, there is a consistent decline in the values to  $0.33\text{Scm}^{-1}$ .
- As soon as the cooling process starts there are no more uncontrolled twisting of polymer chains. The whole film now behaves as a stable single-phase network of semiconductors. With decreasing temperature, the activation energy of thermal transitions decreases.



2(a)



2(b)

Figure: Conductivity vs Temperature

## CHAPTER 5

### CONCLUSION

#### **5.1 Conclusion**

We were successfully able to synthesize Tin Selenide using the Solvothermal method as confirmed by the XRD analysis and there is no phase change. The crystallite size is calculated to be 120.68nm with help of W-H plot. Analysis of electrical, thermal and thermoelectric performances was also conducted using appropriate methods mentioned in Chapter 4. Overall, the fabrication of Tin Selenide was perfectly done and it was used as a dopant for the synthesis of flexible thermoelectric polymer thin films.

The synthesis of the flexible thin films was also done correctly as confirmed by the XRD analysis. The electrical performance and the thermal stability of the thin films were also analysed using appropriate methods mentioned in chapter 4. But we were not able to conduct appropriate tests to analyse the thermoelectric performance of these thin films, nor were we able to conduct flexibility/bending test and analyse whether bending the films multiple times changes their properties permanently or not.